2020 IEEE/RSJ International Conference on Intelligent Robots and Systems (IROS)
October 25-29, 2020, Las Vegas, NV, USA (Virtual)

Snapbot V2: a Reconfigurable Legged Robot with a Camera for Self Configuration Recognition

Kevin G. Gim and Joohyung Kim

Abstract— **In this paper, we present the second version of a reconfigurable modular legged robot, Snapbot V2. The mechanical design of Snapbot V2 is enhanced for better dynamic performance and robust connection with modular legs. A motion generator for locomotion is developed to achieve various locomotion skills in one to six-leg configurations. The locomotion is tested on a multi-body dynamic simulation model and implemented on a physical robot as well. A visual detection is implemented with a camera module to recognize the robot's configuration. By detecting the particular color of the parts at the leg module, the robot can recognize the number and location of the connected legs. Based on the recognized configuration, Snapbot V2 selects the proper locomotion style automatically.**

I. INTRODUCTION

Some creatures in Nature are capable of releasing their limbs or tails voluntarily in order to escape from dangerous situations. This behavior is called as self-amputation or Autotomy [1]. By giving up their body parts, the creatures can increase the chance of survival from life-threatening dangers. In addition, the creatures have an ability to adapt their behavior for the new configurations in a short time. Harvestmen, a kind of arachnids, can deliberately detach a leg or even multiple legs without losing its locomotion capability [2]. Many different kinds of insects can also shift their walking pattern in the case of leg amputation [3].

Inspired by this feature of Nature, various robotic systems have been developed to change their configurations and adjust locomotion skills accordingly [4]–[8]. In this research direction, researchers have studied on the modular robots and their problems [4]. Also, some researchers designed multiple locomotion modes for a reconfigurable robot based on its configurations [5]. Jonathan et al. developed a modular self-reconfigurable robot which can adjust the assembly cluster of independent robot units based on the desired tasks autonomously using vision data [8].

A reconfigurable legged robot named Snapbot was created earlier to emulate configuration changes and various styles of legged locomotion [9]. Utilizing magnetic coupling, the modular legs of Snapbot could be attached and detached from its body without any fastener. Snapbot could be changed to 700 configurations with three types of legs and six connection ports at a body. Recognizing the current configuration by itself, Snapbot was able to adapt its locomotion automatically. In this work, only forward walking motion was implemented for one to six leg configuration as an initial verification of the system.

Kevin G. Gim and Joohyung Kim are with the University of Illinois at Urbana-Champign {kggim2, joohyung}@illinois.edu

Fig. 1. Snapbot V2 and its leg modules

In the following studies using Snapbot, researchers focused on testing machine learning methods on a physical robot. Ha et al. conducted a study to develop the locomotion skill of Snapbot using a deep reinforcement learning algorithm [10]. An automated learning system was developed to train crawling gait pattern without manual effort. Another research applied a trajectory-based reinforcement learning method on a physical robot to train four-legged locomotion skills of Snapbot [11]. Three basic locomotion of walking straight, turn left, and right were trained with the proposed sample-efficient method.

In these previous studies, we found some difficulties and limitations of the hardware platform. First, the limited torque capability of Snapbot's actuator is one of the significant constraints for implementing a variety of locomotion skills. Also, a sturdier coupling is required as the legs can be detached in some poses or when there are larger external forces. These problems had been observed more often when applying learning methods with a large number of iterations.

In this paper, we introduce the second version of Snapbot. For the design of Snapbot V2, it is needed to keep the advantages of the previous version and make up for its shortcomings. One big advantage of the previous version is that most of the parts are 3D printed or easy to purchase. Similar to this, Snapbot V2 is designed with 3D printed parts and commercialized parts. And, considering the weakness of the previous version, the design goals for Snapbot V2 has been set to:

- **Reliable connection between main body and each leg**
- **Enough joint torques for fast locomotion**
- **Implementation of basic locomotion skills**
- **Vision-based self-configuration recognition**

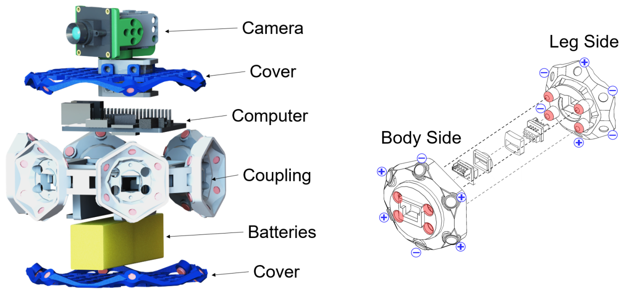

(a) Body (b) One coupling

Fig. 2. Exploded views of body and coupling

This paper is organized as follows. The mechanical design of Snapbot V2 is presented in section II. A new self-configuration recognition algorithm is explained in Section III. Section IV demonstrates how the foot trajectory is designed by a motion generator for locomotion. Simulation results of the motion generator are presented in Section V, and experiment results on a fabricated robot are presented in Section VI. At last, conclusion and future work are discussed in Section VII.

II. HARDWARE DESIGN

In this section, the detailed mechanical design of Snapbot V2 is explained, focusing on the improved features.

A. Body Design

The body of Snapbot V2 encloses essential components such as a computer, batteries, electrical circuit boards, and a camera module. Fig. 2(a) shows the exploded view of the Snapbot V2 body. An Orange PI Lite 2 single-board computer is adopted to operate Snapbot V2. The computer has a compact length that fits into a body frame but also has computing capability for attaching a vision system to the robot. Underneath the computer, two 11.1 V, 850 mAh Li-Po batteries are placed to power the computer and the connected servo motors. There are six leg connection ports around the circumference of the body. Each port provides connection between the computer and two servo motors at a leg module through 3-line TTL serial communication. Two covers are attached to both top and bottom of the body frame to secure and protect the components inside of the body. The covers can be attached and detached using magnets.

On the top cover, there is a camera module that consists of a camera on a 2-DoF moving platform. The module has an ELP-USBFHD01M-L21 USB 2.0 camera, which is capable of capturing 320×240 pixel resolution images. Two Dynamixel XL-320 servo motors are rotating the camera module in the yaw and pitch directions. By controlling the moving platform, Snapbot is able to see its own body and surroundings.

The body frame is 3D printed with VeroWhitePlus material on Stratasys Objet260 Connex Polyjet printer.

The body width is 134 mm measured from the end of a port to the other port at the opposite side. Also, The body height, from the top cover to bottom cover, is 61.55 mm. The weight of the body including all the components is 543 g.

B. Coupling Design

A modular legs can be attached and detached to a body port without any fasteners using a coupling mechanism. In the previous version of Snapbot, the connection between a modular leg and a body frame mainly relied on the magnetic couplings. Since there was no other supporting structure but the rectangular socket walls, the connection could be wobbled and dropped when it had a large impact force. In the coupling of Snapbot V2, four pegs and four mating holes are added at the leg side and the body side respectively, to improve the connection stability. The peg-hole structure is shown in Fig. 2(b) marked with red color. When a leg is inserted to the port, the peg-hole structure establishes a sturdy mechanical coupling that can be maintained under external disturbances. The shape of the port socket is changed to a hexagonal shape. The hexagonal socket can maintain connection at higher axial torsion. Besides, it allows more number of magnets to be installed at the port socket for the stronger magnetic coupling. Six cylindrical (6.4 mm diameter, 6.4 mm height) N48 neodymium magnets are placed at the vertexes of the hexagonal socket. The electrical coupling is unchanged from that of the previous version which is composed of a 8-pin spring-loaded connector and a custom PCB [9].

C. Leg Design

The leg of Snapbot V2 is designed to improve its locomotion capability than that of the previous version. Two Dynamixel XM430-W210-T servo motors are employed to actuate a modular leg, which have the stall torque of 3.0 Nm while that of Snapbot V1's motor is 0.39 Nm. The linkages of the modular leg are 3D printed as well as the body frame. The leg parts are printed with ABS plastic on a Dimension 1200 FDM 3D printer, not on the Polyjet printer used to print the body frame because the leg linkages are exposed to heavier load and impact than the body frame. The leg printed with VerowhitePlus material shows a shorter lifespan as cracks occur due to repetitive impact. On the other hand, the parts printed on the FDM printer show better durability but also taking less cost for printing. In addition, the parts can be printed with various coloring on the FDM printer. The last link and the adjacent parts of the leg are printed in orange color, and the rest of the leg parts are printed in blue color. The purpose of printing the parts in two different colors is to distinguish the parts using a color detection algorithm. A capsule-shape foot is covered with a rubber cap to protect the structure and increase grip at the foot.

Fig. 3(a) presents a 2-DoF Yaw-Pitch Leg with the range of motion limits. The servo motor proximal to the body makes Yaw motion, and the other servo makes pitch motion. In order to match foot trajectory to stepping-like motion, a four-bar linkage mechanism is applied to the pitch motion part. The total weight of a Yaw-Pitch leg is 308 g.

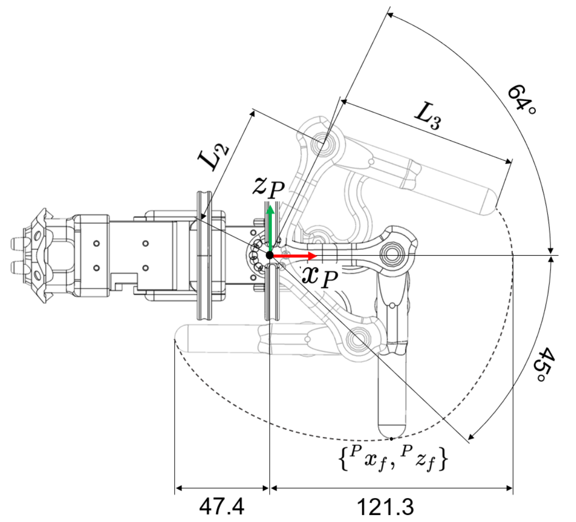

(a) Side view of a Yaw-Pitch leg. Length units in mm. L_2 = 60 mm, L_3 = 85 mm

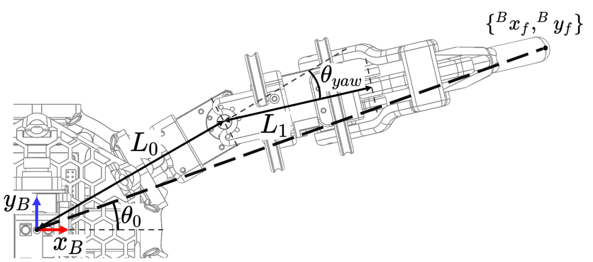

(b) Top view of a Yaw-Pitch leg attached to a body. L_0 = 119.75 mm, L_1 = 56.75 mm.

Fig. 3. Side and Top views of a Yaw-Pitch leg

D. Body Design

1) Four-bar Linkage: The four-bar Linkage mechanism is applied to make a step-like motion of a foot. Fig. 3(a) shows a foot trajectory with a dotted line resulted by the pitch motor rotation. Due to the non-linear geometric relationship of the four-bar linkage mechanism, it is challenging to obtain an analytical solution of the 1-DoF motor angle for a desired position. As an alternative approach, a constraint equation is established to couple two position component, $\{^P x_f,\ ^P z_f\}$ the foot position with respect to the pitch motor rotation axis. By fitting the foot trajectory with a 20^{th} polynomial, a constraint equation can be obtained to express $^P z_f$ as a function of $^P x_f$. Then the pitch motor angle is calculated for the desired $^P x_f$ using the constraint equation. The pitch motor angle θ_{pitch} can be obtained as following equation:

$$\theta_{pitch} = \frac{\operatorname{acos}(L_2^2 + r^2 - L_3^2)}{2rL_2} + \operatorname{acos}\frac{^P z_f}{r}$$

where $r = \sqrt{{^P x_f}^2 + {^P z_f}^2}$.

2) Entire Yaw-Pitch Leg: The joint angle of the two servos can be calculated from the desired foot position with respect to the body coordinate frame, $^B x_f$ and $^B y_f$. The yaw motor angle can be calculated as:

$$\theta_{yaw} = \operatorname{atan2}\left((^B x_f - L_0 \cos\theta_0), (^B y_f - L_0 \sin\theta_0)\right)$$

By knowing the θ_{yaw}, $\{^P x_f,\ ^P z_f\}$ can be calculated and the pitch motor angle θ_{pitch} is obtained through the same process addressed above in the four-bar linkage section.

III. Self Configuration Recognition

Snapbot V2 has to recognize the the number and location of the connected modular legs to select an appropriate locomotion style. Each servo motor in the six modular legs has a unique motor ID in a number between 1 to 12 without overlapping. As all the servo motors are joined in a serial communication hub, the number and ID of connected motors can be collected by scanning the serial communication port. Although the motor IDs can be recognized through the serial port scanning, the locations of each modular leg still need to be recognized.

Snapbot V1 observes the current of the servo motor data line to identify which motor is connected to which port. In Snapbot V2, the location of the leg is visually recognized as a camera module is newly attached to the system.

The camera module consists of a camera and a 2-DoF moving platform. The platform is manipulated to see an individual port at the body. When the camera captures an image of a port, color detection algorithm is implemented to to find an object from the image. The RGB data of each pixel are extracted from the image which has 320×240 pixel resolution. Then the algorithm counts the number of pixels having the RGB values within the desired color threshold

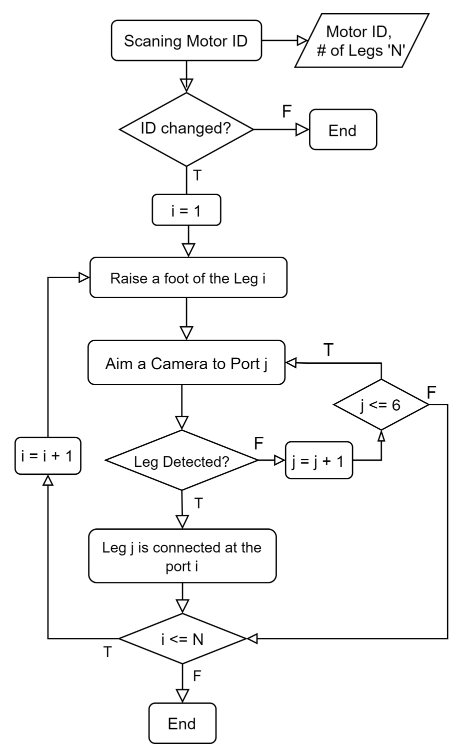

Fig. 4. Full configuration recognition algorithm

range. If there are more number of pixels than a pixel number threshold, the algorithm knows that a target object presents in the captured image. There are two different cases for the configuration recognition; 1) When a robot loses or obtains a leg with the knowledge of its past configuration. 2) When the robot has no information about its past configuration.

In the first case self-configuration recognition can be done promptly since the robot knows the current configuration. When legs are disconnected from the robot, the disconnected one can be identified by comparing the list of new motor IDs and old motor IDs. On the other hand, when a leg is newly added, the IDs of new leg can be found with the serial port scanning but still it is necessary to identify the port where the new leg is just connected. In order to find the leg location, the 2-DoF camera module is activated to capture image of individual ports. Since the robot knows which ports were unoccupied, the camera module only captures images of the empty ports. From the captured images, the color detection algorithm look for the blue-colored part of the leg to distinguish the newly occupied port.

In the second case, the robot has to identify its configuration from scratch. The full recognition is required in such cases when the system is started up with some connected legs, or more than one leg is added to the body simultaneously. A flowchart diagram of the full recognition algorithm is demonstrated at Fig. 4. After scanning the serial communication port, the system acquires the ID of connected servos. The color detection algorithm is used to identify which leg is connected to which port. Instead of detecting blue-colored part, the camera capture the orange-colored parts of the leg. When the foot is not raised, only the blue-colored parts are visual when the camera captures image of the port with a leg. As the foot is raised, the orange-colored parts are exposed and the leg with the raised foot can be distinguished from the other legs. The leg module with smallest motor IDs raises its foot first, then the camera module captures the image of the port from the port one to six in turn until it finds the orange-colored part. Once the color detection algorithm identifies the location of the first leg, the same process is repeated until the location of all the connected legs are recognized. After configuration recognition is completed, the robot adapts the locomotion style accordingly.

IV. LOCOMOTION

The first version Snapbot was able to perform a forward-moving motion for one to six-leg configurations. Rowing or crawling motion were applied when the number of connected legs were not sufficient to lift the body. When more than four legs were connected, a trot walking motion was applied. The locomotion skill was only limited to move straight forward. In Snapbot V2, a motion generator is introduced to compose the foot step trajectory for various locomotion skills.

The walking motion of multi-legged robots consists of swing phase and stance phase [12]. During the swing phase, a foot is lifted and projected from a Posterior Extreme Position (PEP) to an Anterior Extreme Position (AEP) following a elliptical line on a sagittal plane. When the foot is touching the ground, the foot is retracted following a straight line to the PEP while maintaining contact with the ground during the stance phase. A propelled direction of a body is determined by direction of the line connecting the AEP and PEP.

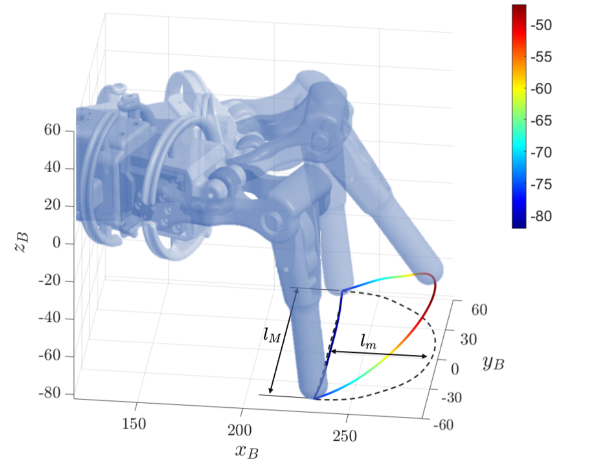

Fig. 5. 3D plot of the foot position (colored-line) of the right middle leg in the six-leg configuration while tracking the semi-ellipse trajectory (dotted-line) on the bottom plane.

TABLE I

LOCOMOTION COMMAND VARIABLES

Variable	Description
l_M	Major length of the semi-ellipse foot trajectory. Step length
l_m	Minor length of the semi-ellipse foot trajectory.
T_s	Period of the one step cycle.
θ_t	Translation angle when the robot is walking diagonally.
α	Step length difference between left legs and right legs
β	rotating in place enable parameter. 0 or 1.

Due to the limited DoF of the modular leg, the foot of Snapbot V2 is tracking a semi-ellipse trajectory drawn on a bottom plane (XY plane) of the body, but not on a sagittal plane (XZ plane) while walking. The foot is raised when it is passing a ellipse segment during the swing phase. The four-bar linkage mechanism allows the foot have a small height change during the stance phase, so the foot can maintain contact with the ground. Fig. 5 presents the desired foot trajectory on the bottom plane and the resulting foot position trace while tracking the trajectory.

Table. 1 presents the locomotion command variables that consist the foot trajectory. The foot trajectory can be designed to achieve a desired locomotion skill by adjusting the variables. The foot trajectory of a leg can be expressed as the following equation.

$$\begin{bmatrix} {}^B x_f \\ {}^B y_f \end{bmatrix} = \left((1-\beta)^B R_z(\theta_t) \begin{bmatrix} 1 & 0 \\ 0 & 1 \pm \alpha \end{bmatrix} + \beta^B R_z(\theta_0 - \frac{\pi}{2}) \right) \begin{bmatrix} x_s \\ y_s \end{bmatrix} + \begin{bmatrix} {}^B x_0 \\ {}^B y_0 \end{bmatrix}$$

Where ${}^B R_z$ is a rotation matrix, and $[{}^B x_0, {}^B y_0]^T$ is a initial position of the foot with respect to the body frame. $[x_s, y_s]^T$ is a vectors representing a semi-ellipse trajectory expressed as the equation below.

$$x_s = \begin{cases} \frac{l_m}{2}\cos\frac{2\pi}{T_s}t & x_s \geq 0 \\ 0 & x_s < 0 \end{cases}$$
$$y_s = \frac{l_M}{2}\sin\frac{2\pi}{T_s}t$$

Various locomotion skills can be achieved by adjusting the locomotion command variables. When α and θ_t equal to zero, the robot is walking straight forward. If $\theta_t \neq 0$, the robot can walk diagonally as the legs propel the body to a diagonal direction with angle θ_t while the body is still facing the anterior direction. α can be used to steer the walking direction of the robot. If legs at one side has larger step length than the legs at the opposite side, the heading direction of the robot can be tilted towards the side being propelled less. When $\beta = 1$, the AEP and PEP of each step trajectory are placed on a circle having an origin at the center of a body and the robot can rotate the body in place. β prevents the overlapping of walking locomotion and rotating in place locomotion.

Snapbot V2 selects appropriate locomotion style according to the recognized configuration. Similar with the locomotion of Snapbot V1, rowing and crawling locomotion is selected for one to three-leg configurations. When four to six legs are connected, multi-leg walking locomotion is applied to walk with a fully lifted body. The following section explains how the four-leg and six-leg locomotion are implemented.

A. Four-Leg Locomotion

There are three possible configurations when the robot has four legs connected among six ports at the body. In this paper, the locomotion was developed for a symmetric four-leg configuration. The direction pointing one of the empty ports is set to the anterior direction of the robot. A trot gait is selected as a gait pattern of the four-leg configuration. In the trot gain, two legs in diagonal become a pair driven together, while the other pair are moving together with a phase offset of a half cycle. Thus, when one pair is in the swing phase, the other pair is in the stance phase.

B. Six-Leg Locomotion

There is only one configuration when all the six leg modules are connected. In this case, the anterior direction is set to the middle of the first port and the sixth port. And a tripod gait is selected as a gait pattern which resembles the gait pattern of insects. Three legs (front and rear legs at one side, and middle leg at the other side) moves together with the same step cycle. While one group of three legs is in the swing phase, the other group is in the stance phase by having a half-cycle phase offset. In this gait, the body is always supported by three legs which prevent the robot from losing balance.

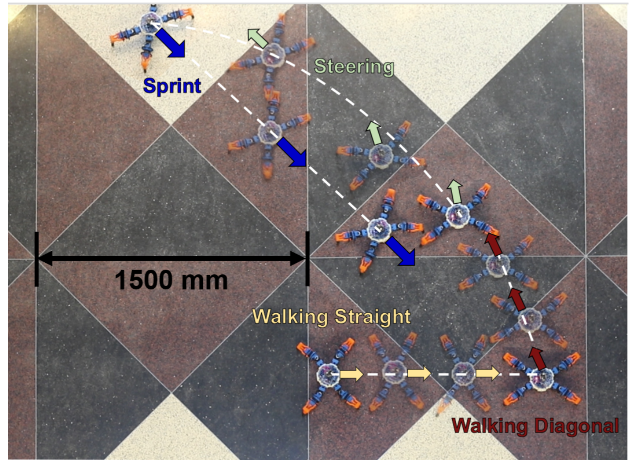

Fig. 6. Snapshots of the four-leg configuration locomotion experiments. Snapbot V2 is performing walking straight, walking diagonal, steering, rotation in place, and sprint. The length of a single tile is 1500 mm.

V. Simulation Result

The motion generator was tested on a simulation model using MATLAB Simscape multi-body simulation. Using the simulation model, the maximum step length and step period of the each configuration were found by considering the saturation of torque and speed capability of the servo motor provided by the manufacturer.

In the four-leg configuration, the largest step length was limited to 70 mm to keep the robot balanced. By constraining the saturation of torque and speed of the servo motors, the maximum forward walking speed and maximum yaw rotation speed were estimated. The resulting maximum forward walking speed was 280 mm/s at 70 mm step length and 0.5 s step period. Also, the maximum Yaw rotation speed was estimated as $56.17°/s$.

Snapbot V2 in the six leg configuration took larger step length and faster step period than the other configurations. The robot was able to take the maximum step stoke of 100 mm without losing balance. In the six-leg configuration, the maximum forward walking speed was estimated as 500 mm/s at 100 mm step length and 0.4 s step period. The estimated maximum Yaw rotation speed was obtained as $103.7°/s$ through the simulation.

VI. Hardware Experiment

The locomotion of four-leg and six-leg configuration were validated on a physical robot hardware. Fig. 6 demonstrates the snapshots of Snapbot V2 in the four-leg configuration performing walking straight, walking diagonal, yaw rotation in place, steering, and sprint with maximum speed in sequence. The robot was remotely controlled via SSH network connection.

The motor position command and measurement during the six-leg sprint motion are presented in Fig. 7. Note that the left front foot and left middle foot have a phase delay of a half cycle. As presented in the plots in first column, the robot can track the reference trajectory of 0.4 s step period with

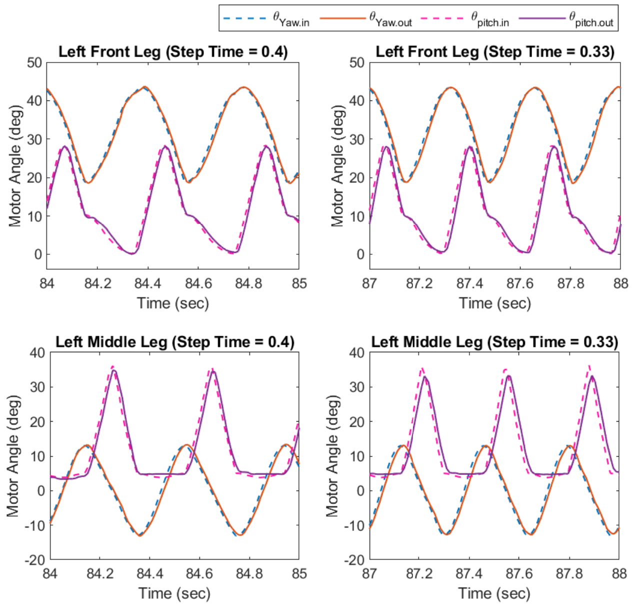

Fig. 7. Motor input/output during the maximum speed sprint motion on the six-leg configuration. The step period is 0.4 s in the first column and 0.33 s in the plots in second column.

100 mm step length. With the faster step period of 0.33 s, the pitch motor of the left middle leg shows tracking error. The robot was able to achieve the maximum sprint speed of 474.92 mm/s, calculated by analysing each frame of the video. In the four-leg configuration, Snapbot V2 achieved 0.5 s step period, 70 mm step length. The resulting sprint speed was measured as 265.16 mm/s.

The self-configuration recognition algorithm was also verified on a physical robot. When the robot system starts up, it initially recognized the configuration. After the current configuration was recognized, the robot selected a proper locomotion style for one to six-leg configuration accordingly. The robot scanned the serial port with a regular interval of 100ms to detect configuration change promptly while the system was running. Whenever the configuration was changed, the system entered to recognition mode. The implementation of self-configuration recognition is demonstrated in a supplement video.

VII. CONCLUSION AND FUTURE WORK

In this paper, we presented a reconfigurable legged robot, Snapbot V2, which made up for the weak points found in applications of the previous version robot. The mechanical design of the robot was enhanced to have a better dynamic performance. The coupling design was changed to have more reliable connections between its body and legs under heavy loads and impact force. A camera module with 2-DoF moving platform was added to the body for the self-configuration recognition. With this camera, we implemented a method to recognize which leg is attached to which port by using color detection. The motion generator for locomotion was developed to compose the foot step trajectory of each foot for the desired locomotion skill. Various locomotion skills were implemented such as walking straight and diagonal, steering, and rotation around the body center. All the developed methods for Snapbot V2 ware tested in the simulation and the hardware.

We are planning to make more legs with different configurations, to find which design is better for the locomotion. Also, we will continue exploring the reinforcement learning methods to tackle the real-world learning problems in legged robots. With the attached camera, Snapbot V2 is now able to see its surroundings, which will open up possibilities to various research directions.

ACKNOWLEDGMENT

We express our gratitude to RuthAnn Haefli, Alexandra Brown, and Prof. Molly H. Goldstein for helping us to fabricate parts of Snapbot V2 in the Product Design Lab at University of Illinois, Urbana-Champaign.

REFERENCES

[1] Z. Emberts, C. W. Miller, D. Kiehl, and C. M. St. Mary, "Cut your losses: self-amputation of injured limbs increases survival," *Behavioral Ecology*, vol. 28, no. 4, pp. 1047–1054, 04 2017.

[2] M. Domínguez, I. Escalante, F. Carrasco-Rueda, C. E. Figuerola-Hernández, M. M. Ayup, M. N. Umaña, D. Ramos, A. González-Zamora, C. Brizuela, W. Delgado *et al.*, "Losing legs and walking hard: effects of autotomy and different substrates in the locomotion of harvestmen in the genus prionostemma," *The Journal of Arachnology*, vol. 44, no. 1, pp. 76–82, 2016.

[3] D. M. Wilson, "Insect walking," *Annual review of entomology*, vol. 11, no. 1, pp. 103–122, 1966.

[4] M. Yim, W. Shen, B. Salemi, D. Rus, M. Moll, H. Lipson, E. Klavins, and G. S. Chirikjian, "Modular self-reconfigurable robot systems [grand challenges of robotics]," *IEEE Robotics Automation Magazine*, vol. 14, no. 1, pp. 43–52, March 2007.

[5] Wei-Min Shen, M. Krivokon, Harris Chiu, J. Everist, M. Rubenstein, and J. Venkatesh, "Multimode locomotion via superbot robots," in *Proceedings 2006 IEEE International Conference on Robotics and Automation, 2006. ICRA 2006.*, May 2006, pp. 2552–2557.

[6] A. Gapchup and A. Wani, "Flying rubick's with self assembling using m-blocks," in *2017 International Conference on Inventive Systems and Control (ICISC)*, Jan 2017, pp. 1–6.

[7] K. Støy, W. M. Shen, and P. Will, "How to make a self-reconfigurable robot run," in *Proceedings of the First International Joint Conference on Autonomous Agents and Multiagent Systems: Part 2*, ser. AAMAS '02. New York, NY, USA: Association for Computing Machinery, 2002, p. 813–820.

[8] J. Daudelin, G. Jing, T. Tosun, M. Yim, H. Kress-Gazit, and M. Campbell, "An integrated system for perception-driven autonomy with modular robots," *Science Robotics*, vol. 3, 09 2017.

[9] J. Kim, A. Alspach, and K. Yamane, "Snapbot: A reconfigurable legged robot," in *2017 IEEE/RSJ International Conference on Intelligent Robots and Systems (IROS)*. IEEE, 2017, pp. 5861–5867.

[10] S. Ha, J. Kim, and K. Yamane, "Automated deep reinforcement learning environment for hardware of a modular legged robot," in *2018 15th International Conference on Ubiquitous Robots (UR)*. IEEE, 2018, pp. 348–354.

[11] S. Choi and J. Kim, "Trajectory-based probabilistic policy gradient for learning locomotion behaviors," in *2019 International Conference on Robotics and Automation (ICRA)*. IEEE, 2019, pp. 1–7.

[12] F. Tedeschi and G. Carbone, "Hexapod walking robot locomotion," in *Motion and Operation Planning of Robotic Systems: Background and Practical Approaches*, ser. Mechanisms and Machine Science. Springer International Publishing, 2015, pp. 439–468.